Chronology of the Bayo River valley deglaciation and implications for the Late Pleistocene Atlantic-to-Pacific drainage reversal of the General Carrera-Buenos Aires palaeolake, Patagonia-Chile

Germán Aguilar, Joseph Martinod, Matías Gallardo, Christian Sue

Andean Geology 50 (1): 1-21. January, 2023
doi: 10.5027/andgeoV50n1-6460

Andean Geology
www.andeangeology.cl

Chronology of the Bayo River valley deglaciation and implications for the Late Pleistocene Atlantic-to-Pacific drainage reversal of the General Carrera-Buenos Aires palaeolake, Patagonia-Chile

***Germán Aguilar[1], Joseph Martinod[2], Matías Gallardo[3], Christian Sue[2]**

[1] *Advanced Mining Technology Center, Facultad de Ciencias Físicas y Matemáticas, Universidad de Chile, Avda. Tupper 2007, Santiago, Chile.*
german.aguilar@amtc.uchile.cl

[2] *ISTerre, University Grenoble Alpes, University Savoie Mont Blanc, CNRS, IRD, IFSTTAR, 1381 rue de la piscine, 38400 Saint Martin d'Hères, France.*
joseph.martinod@univ-smb.fr; christian.sue@univ-grenoble-alpes.fr

[3] *Departamento de Geología, Facultad de Ciencias Físicas y Matemáticas, Universidad de Chile, Avda. Tupper 2007, Santiago, Chile.*
matias.gallardo.heck@gmail.com

***** *Corresponding author: german.aguilar@amtc.uchile.cl*

ABSTRACT. We present a study on the glacial and paraglacial geomorphology of a Patagonian Cordillera Valley that is key to understanding evolution of the great lakes of Patagonia. ^{10}Be cosmogenic nuclide exposure ages of ice-moulded surfaces from the Bayo River Valley confirm that the valley became ice-free before 13.4-14.2 ka. This valley constituted the first outlet of the Chelenko Lake, precursor of the General Carrera-Buenos Aires Lake (GCBAL), toward the Pacific Ocean. This age constrains the timing of the lake drainage reversal from the Atlantic Ocean to the Pacific Ocean. Alluvial fans and terrace levels recognized in the eastern segment of the valley at the same altitude as terrace levels observed in the GCBAL basin confirm that the Bayo Pass controlled the elevation of the lake once the drainage reversed to Pacific Ocean. ^{10}Be cosmogenic nuclide exposure ages also confirm that the maximum advance of the Exploradores Glacier since its major retreat >13.4-14.2 ka ago occurred during the Little Ice Age, the last remnant of glacial drift in these valleys.

Keywords: Deglaciation chronology, Paleolake history, Patagonia-Chile.

RESUMEN. Cronología de la deglaciación del valle del río Bayo e implicaciones para la inversión del drenaje del Atlántico al Pacífico del Pleistoceno tardío en el paleolago General Carrera-Buenos Aires, Patagonia-Chile. Presentamos un estudio sobre la geomorfología glacial y paraglacial de un valle de la Cordillera Patagónica que es clave para entender la evolución de los grandes lagos de la Patagonia. Edades de exposición cosmogénica de ^{10}Be de las superficies moldeadas por el hielo del valle del Río Bayo confirman que este quedó libre de hielo antes de 13,4-14,2 ka y constituyó la primera vía de drenaje del lago Chelenko, precursor del lago General Carrera-Buenos Aires (LGCBA), hacia el Océano Pacífico. Esta edad limita el momento de la inversión del drenaje del lago desde el Océano Atlántico hacia el Océano Pacífico. Los abanicos aluviales y los niveles de las terrazas reconocidos en el segmento oriental del valle, a la misma altura que los niveles de las terrazas observados en la cuenca del LGCBA, confirman que el Portezuelo del Bayo controló la elevación del lago una vez que el drenaje se invirtió hacia el Océano Pacífico. Las edades de exposición cosmogénica de ^{10}Be también confirman que el máximo avance del glaciar Exploradores, desde su mayor retroceso hace >13.4-14.2 ka, ocurrió durante la Pequeña Edad de Hielo, último remanente de la deriva glaciar en estos valles.

Palabras clave: Cronología de la deglaciación, Historia de los paleolagos, Patagonia-Chile.

1. Introduction

The General Carrera-Buenos Aires Lake (GCBAL, Fig. 1) area is one of the Chilean Patagonia regions where the geomorphological evolution associated with hydro-climatic changes during the late Pleistocene/Holocene deglaciation has been best studied (Rabassa and Clappert, 1990; Davies *et al.*, 2020 and references therein). The depression in which the GCBAL lies has been carved out by a major glacial lobe flowing eastward from the ice cap that covered the Patagonian Cordillera during Pliocene and Pleistocene glacial periods (*e.g.*, Turner *et al.*, 2005; Bell, 2008; Bendle *et al.*, 2017b; Davies *et al.*, 2020). During the deglaciation that followed the Local Last Glacial Maximum (LLGM; 27-20 ka), previously ice-covered surfaces were exposed, and proglacial lakes were generated. These lakes are the precursors of the current GCBAL (*e.g.,* Caldenius, 1932; Turner *et al.*, 2005; Thorndycraft *et al.*, 2019). Many geomorphological studies focused on the description and dating of the glacial deposits (*e.g.*, Douglass *et al.*, 2006; Kaplan *et al.*, 2004), pro-glacial and lacustrine deposits (*e.g.,* Bendle *et al.*, 2017a; Turner *et al.*, 2005; Vásquez *et al.*, 2022) associated with the LLGM and deglaciation that border the great lakes of the eastern Patagonian Cordillera foothills (*e.g.*, GCBAL). For example, Bendle *et al.* (2017b) show detailed geomorphological maps of these landforms. On the contrary, little attention has been given to the geomorphological evolution of the Patagonian Cordillera valleys in which the action of glaciers was essentially erosive.

Following the beginning of glacial retreat, major lakes occupied the main valleys that had been carved in the eastern sector of the Patagonian Cordillera (Bendle *et al.*, 2017a). The evolution of lake levels has been controlled by glacial activity in the Patagonian Cordillera valleys after the last 18 ka-old major glacial retreat (Glasser *et al.*, 2016; Bendle *et al.*, 2017a; Thorndycraft *et al.*, 2019). At first, these lakes drained toward the Atlantic Ocean since the icecap was damming all possible outlets toward the Pacific Ocean. During this period paleo-shorelines (T2 terraces and paleoshores) formed approximately 230 m above the present-day GCBAL lake level (Turner *et al.*, 2005; Martinod *et al.*, 2016; Thorndycraft *et al.*, 2019; Isla and Espinoza, 2021). This precursor of the GCBAL has been named Deseado Lake by Thorndycraft *et al.* (2019). Elevation of T2 paleo-shorelines indicates that during this stage the lake was flowing toward the Atlantic Ocean through an outlet located close to the Perito Moreno Pass in Argentina.

A major level of T1 paleo-shorelines is preserved everywhere around the GCBAL, approximately 140 m above the present-day lake level. These paleoshorelines indicate that the level of the lake stabilized at an intermediate elevation, before dropping to its current level. Paleoshorelines are also visible at similar elevations around the present-day Cochrane-Pueyrredon Lake to the South, suggesting that the ancient lake was unifying the present-day GCBAL and Cochrane-Pueyrredon Lake (Turner *et al.*, 2005; Vásquez *et al.,* 2022). This unified lake has been named Chelenko Lake by Davies *et al.* (2018) and Thorndycraft *et al.* (2019). Lake Chelenko did not flow towards the Atlantic Ocean since its elevation was lower than all possible outlets to the East, either from their Southern and Northern branches.

Martinod *et al.* (2016) proposed that the Bayo River Valley (BRV) was draining the Chelenko Lake toward the Pacific Ocean during the formation of the prominent lacustrine terrace level (T1) in the shores of the current GCBAL. Indeed, the minimum elevation of the water divide (Bayo Pass) between the BRV and the GCBAL watershed corresponds to the level of the Chelenko Lake. Thorndycraft *et al.* (2019) applied bayesian models based on a range of geochronological data, to infer that Chelenko Lake was extant between 15 and 12.6 ka. They propose that this lake was flowing through the BRV because the Baker River Valley outlet was dammed by a still coalescent ice sheet joining the present-day Northern and Southern Patagonian Ice fields. This is evidenced by cosmogenic nuclide exposure ages of the Bertrand Lake moraines (Davies *et al.*, 2018), showing that the Baker River Valley, current outlet of GCBAL and Cochrane-Pueyrredon Lake, was blocked during the Antarctic Cold Reversal (ACR; 14.5-12.9 ka; Jouzel *et al.*, 2001), *i.e.*, after the lake level fall from T2 (Deseado) to T1 (Chelenko).

In contrast, Bourgois *et al.* (2016a, 2016b, 2019) consider that the BRV could not have been the Chelenko Lake outlet because it was still blocked by a glacier tongue coming from the Northern Patagonian Ice Field at that moment. Glasser *et al.* (2006), indeed, argue that the Northern Patagonian Ice Field was still occupying the BRV ~10 ka ago. Then, in the absence of any existing outlet, Bourgois *et al.* (2016a) propose

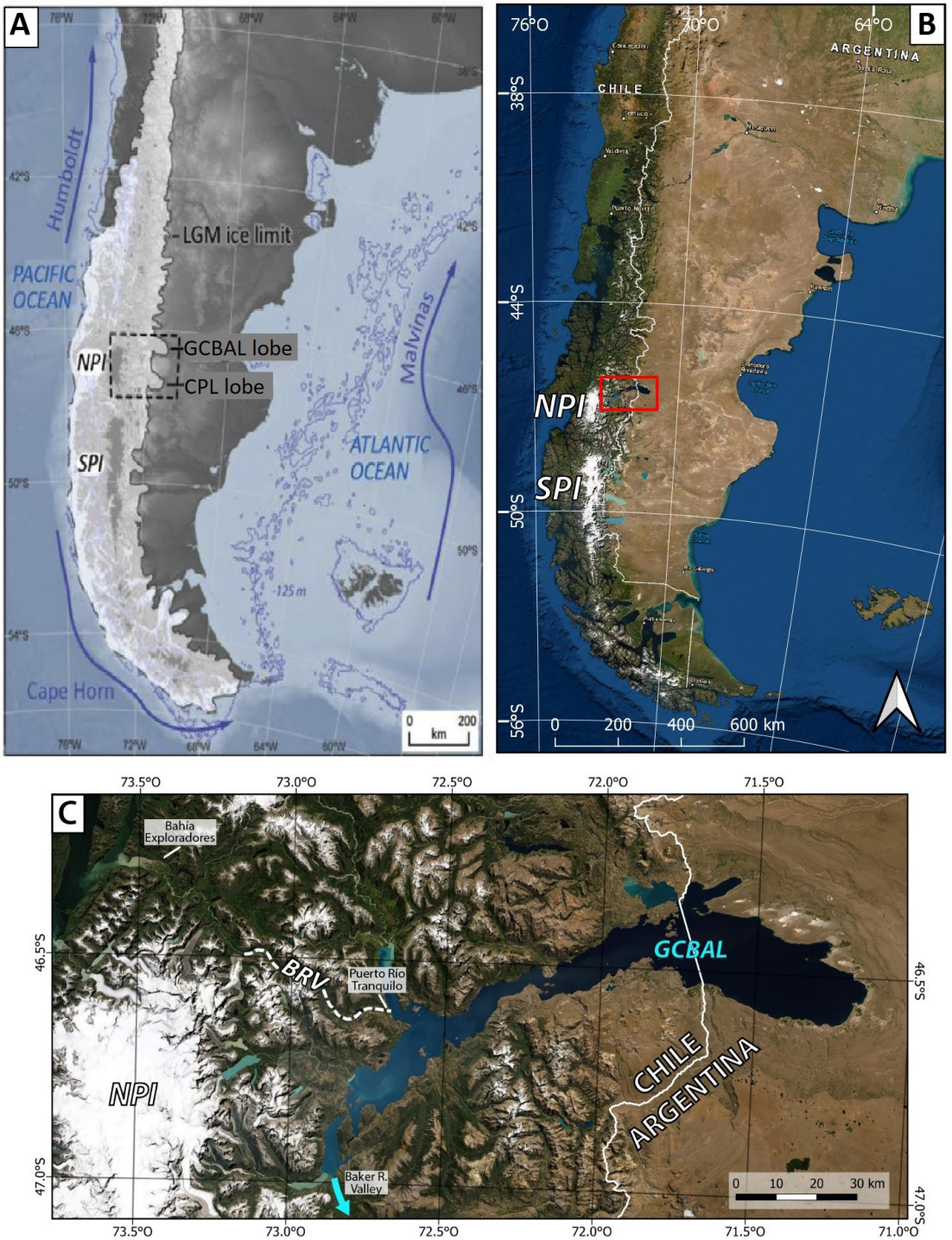

FIG. 1. **A.** Last Glacial Maximum (LGM) extent of the Patagonian Ice Fields from Thorndycraft *et al*. (2019). General Carrera-Buenos Aires Lake (GCBAL) and Cochrane-Pueyrredon Lake (CPL) lobes are located. **B.** Current extent of the Patagonian Ice Fields: Northern Patagonian Ice Field (NPI) and Southern Patagonian Ice Field (SPI). The General Carrera-Buenos Aires Lake area is enclosed in a red box. **C.** Location of General Carrera-Buenos Aires Lake, the Bayo River Valley (BRV) and its outlet on a fjord of Pacific Ocean (Bahía Exploradores).

that the T1 terrace-level formed during an endorheic period resulting from a severe rainfall deficit. Within this framework, dating glacial retreat in the BRV is crucial to know if this valley could have drained the Chelenko Lake, and to understand the mechanisms that controlled the paleo-lake levels which, in turn, have major implications for the postglacial climatic evolution of Patagonia and continental-scale lake drainage reversals.

The aim of the study is to date when the valley became ice-free and evaluate the landform evidence to test published paleolake evolution models and the hypothesis that the Bayo River Valley was the drainage pathway of Chelenko Lake. This paper presents geomorphological mapping and new ^{10}Be exposure ages of ice-moulded bedrock surfaces in the BRV that allow us to evaluate the timing of deglaciation of the valley and lake drainage reversal at continental-scale. Based on geomorphological mapping, we study the glacial, paraglacial and fluvial processes that led to the landform record in the valley. The exposure ages of ice-moulded bedrock surfaces are discussed in relation to the age and position of glacier in the valley, and we describe their implications for paleo-lake history.

2. Geomorphology of the studied area

The BRV is located north of the Northern Patagonian Ice Field that still covers part of the Patagonian Cordillera (Fig. 1C). The Bayo River is approximately 40 km long, its catchment area being about 250 km^2. It rises in the Bayo Pass (370 m a.s.l.) and flows westwards into the Bayo Lake (124 m a.s.l.), which is drained by the Exploradores River into the Pacific Ocean (Fig. 2A). The Bayo Pass separates the BRV from the Tranquilo River valley. This latter valley is only 8.5 km long and flows into the GCBAL (210 m a.s.l.).

The pre-Quaternary basement of the BRV is composed of three main units (Sernageomin, 2003). The upper segment of the valley was excavated in the East Andean Metamorphic Complex of Devonian-Carboniferous age (quartz-muscovite schists and phyllites), while the lower segment is excavated in the Patagonian Batholith of Cretaceous age (monzogranites and tonalites). East of the Bayo Pass, in the Tranquilo River valley, some outcrops correspond to the Ibáñez Formation (Mesozoic volcaniclastic sequences). Georgieva *et al*. (2016) proposed that the direction of the valleys coincides with NE verging reverse faults of approximately N120°E strike and high SW dips (50°-80°), derived from the Exploradores Fault Zone.

Three knickpoint are identified in the BRV (KP1, KP2 and KP3 in figures 2 and 3). Between knickpoints KP1 and KP2, the BRV is characterized by a steep longitudinal profile of the thalweg and a narrower valley than upstream and downstream (Fig. 4). KP1 coincides with the contact between the metamorphic complex and the Patagonian Batholith. In contrast, no geological change is observed at KP2 to explain this perturbation in the shape of the valley. This may be explained by glacial re-excavation in the core of the Patagonian Cordillera, where KP2 delimits a zone of high glacial erosion in the past. This greater erosive capacity can be explained by a greater magnitude and/or stationary position of a glacial front, which is possibly due to the longer permanence of the glacier downstream KP2.

Another distinctive feature of this valley is the Bayo Pass (370 m a.s.l.), that separates the BRV from the Tranquilo Valley. It is covered by an active alluvial fan (Fig. 2B) and is the lowest water divide between the eastern watershed, that discharges to the east into the GCBAL, and the western watershed, that discharges to the West into the Bayo Lake. The Bayo Pass separates a zone with Mesozoic sequences (Ibáñez Formation) over the metamorphic complex in the Tranquilo River valley, whereas, west of the Bayo Pass, in the BRV, the Mesozoic sequences do not outcrop and only the metamorphic complex is present as a rocky substrate.

The BRV is now ice-free in the trunk valleys, but previous studies indicate that ice masses covered the whole Patagonian Cordillera during the LLGM (*e.g*., Caldenius, 1932). In fact, two divergent glacier tongues crossed the Patagonian Cordillera: a western tongue via the Exploradores Valley towards the fjords of the Pacific Ocean and an eastern one via the BRV towards the inlets of the large proglacial lakes located east of the Patagonian Cordillera (Davies *et al*., 2020). The eastward drift tongue that covered the BRV had a lower thickness than the western tongue that covered the Exploradores Valley, as the BRV constitutes a narrower glacial valley, hanging and less evolved in cross section than the Exploradores valley (Bennett and Glasser, 2011; Munro-Stasiuk *et al*., 2013). During the LLGM (27-20 ka) the eastern tongue amalgamated with other glaciers to contribute

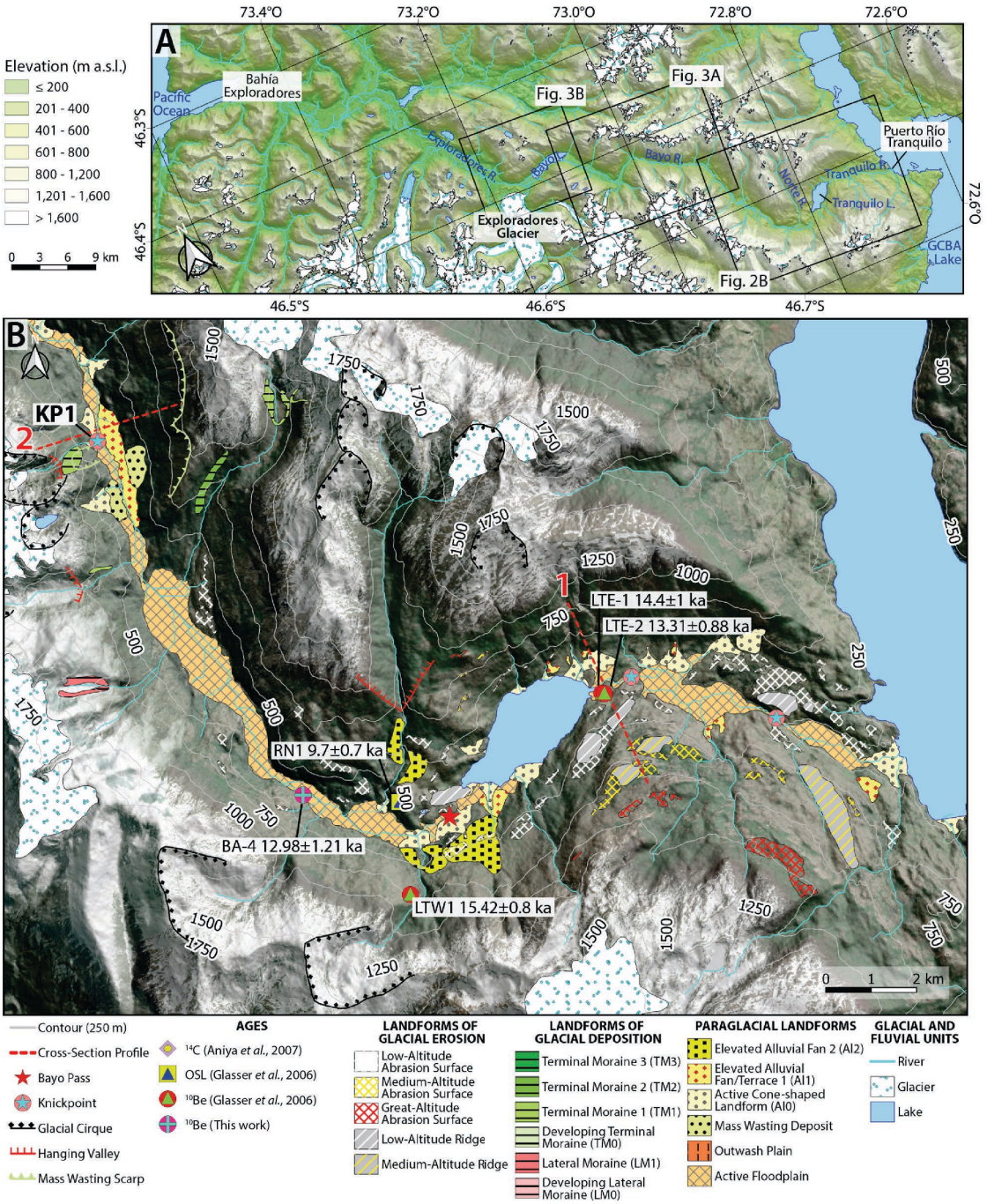

FIG. 2. Geomorphological map of the Bayo River Valley (BRV). **A.** Topography of the studied zone. **B.** Tranquilo River Valley and upper segment of the BRV. Ages come from cosmogenic concentrations measured in this study and in a work by Glasser *et al.* (2006) (recalculated ages). OSL age of alluvial deposit in the Bayo Pass from Glasser *et al*. (2006).

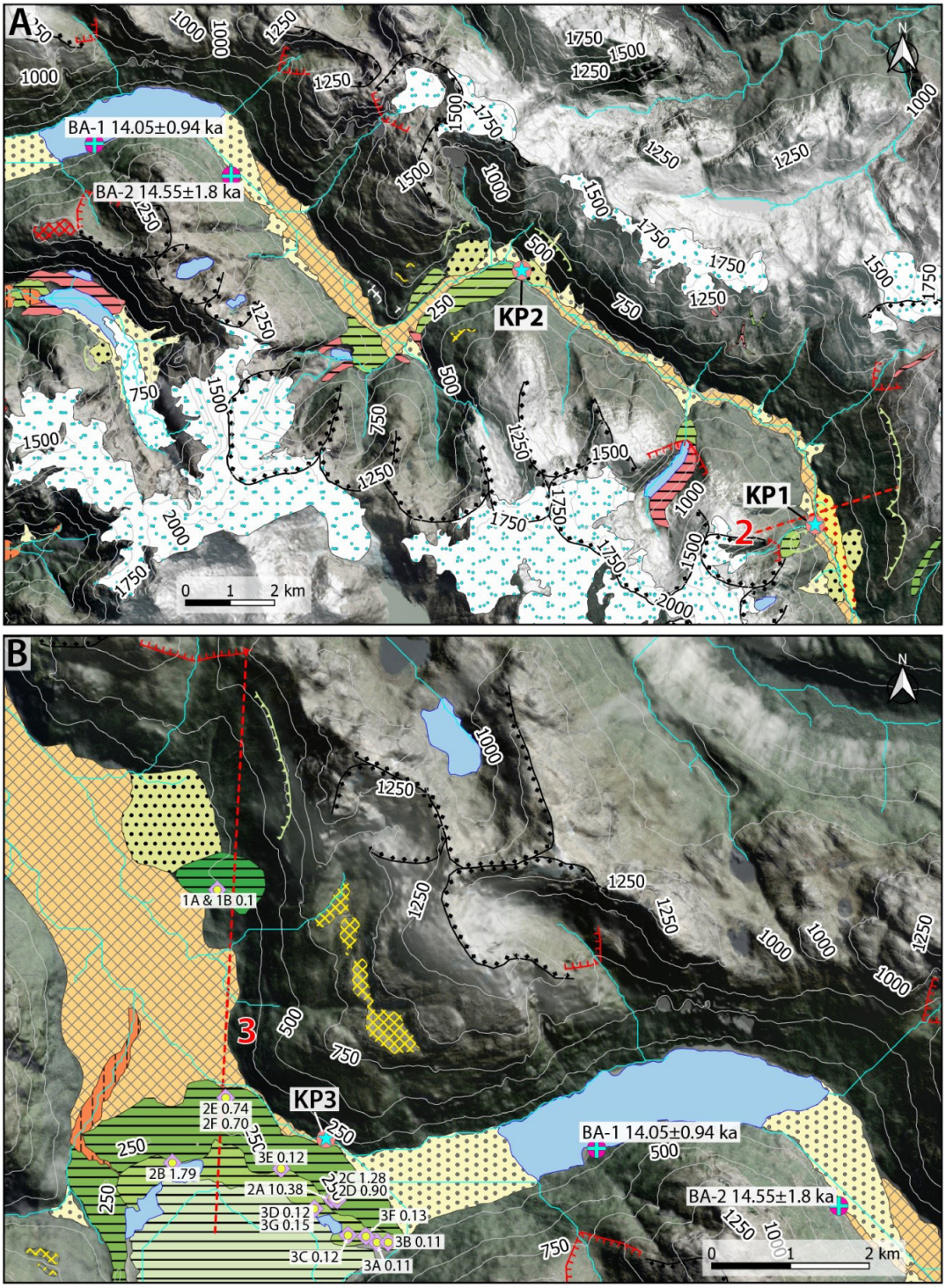

FIG. 3. Geomorphological map of the Bayo River Valley (BRV). **A.** Lower segment of the BRV. **B.** Exploradores Valley. Legend is shown on figure 2. Radiocarbon ages in moraines of the Exploradores Glacier (Aniya *et al*., 2007) calibrated using the OxCal 4.4 program and SHCal20 terrestrial calibration curve (Hogg *et al*., 2020). 2A to 2F radiocarbon ages shown represent the median calibrated age and are expressed in cal. ka BP. More recent ages (<300 yrs; 1A-1B and 3A-3G) are expressed in ka BP.

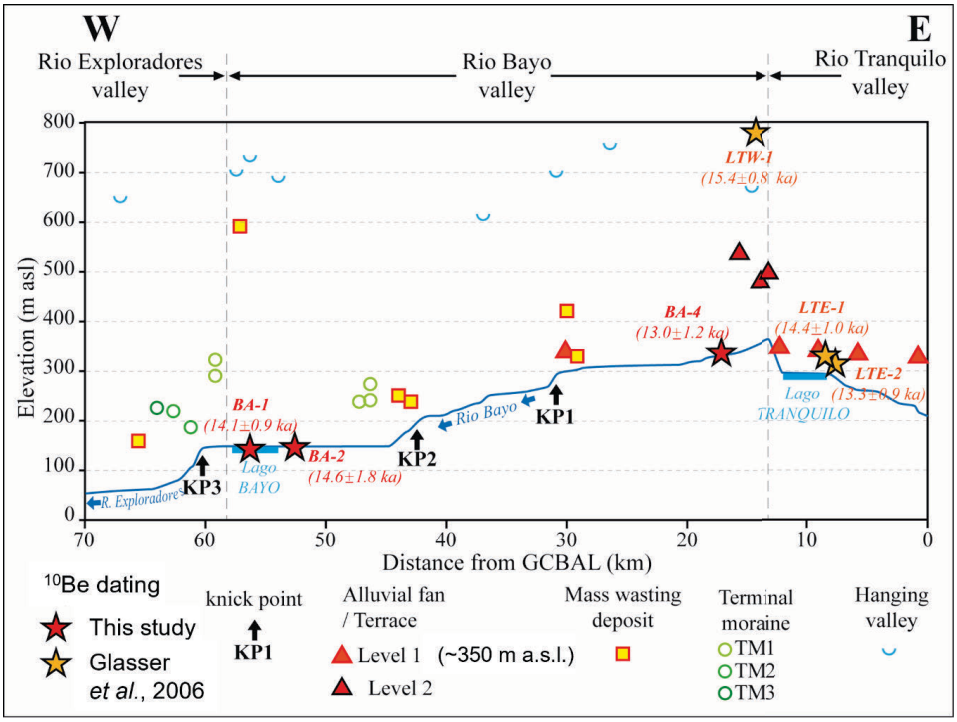

FIG. 4. Thalweg profile with average height of the most relevant landforms recognized in the Tranquilo and Bayo River valleys.

to the glacial lobe that covered the piedmont of the Patagonian Cordillera.

Deglaciation of Patagonian Cordillera was marked by the rapid thinning of the ice cap between 19 and 16 ka ago, which is attributed to a warming of Southern Hemisphere mid to high latitudes, linked to changes in ocean thermohaline circulation, along with a southward migration of westerly winds (Boex *et al*., 2013). Davies *et al*. (2020) suggest that the BRV was filled by a trunk glacier covering the area between Exploradores Glacier and Puerto Tranquilo (Fig. 2A), which remained in the valley until at least 15 ka. However, these authors indicate that during the period between 20-15 ka, ice boundaries in the zone present a low reliability, thus the glacier retreat could have been as early as 17 ka (Mendelova *et al*., 2017).

Fluvial and lacustrine processes developed in the Tranquilo River valley during the Holocene over the previously glacially modelled landscape. Geomorphological mapping and ^{10}Be exposure ages of erratic blocks in the eastern margin of the Tranquilo Lake (LTE1 and LTE2) and one OSL (RN1) age for a fluvio-glacial deposit were published by Glasser *et al*. (2006) (see figure 2B for location). For these authors, corresponding ages mark the retreat of the main glacier coming from the Northern Patagonian Ice Field and flowing eastward in the BRV. According to the original interpretation of Glasser *et al*. (2006), the two ^{10}Be exposure ages (11.4±0.9 and 10.5±0.8 ka, respectively) date the withdrawal of the glacial tongue from the Tranquilo Lake area.

Glasser *et al*. (2012) re-evaluated these ages obtained from concentrations in cosmogenic isotopes at 13.8±0.9 ka. Indeed, after 2006, the in situ ^{10}Be production and half-life had been revised, showing that the cosmic ray exposure ages that were previously estimated were systematically underestimated by ~28% (Bourgois *et al*., 2016a). On the other hand, the OSL age of 9.7 ka in a fluvio-glacial deposit was interpreted as sediment accumulated in the margins of the trunk glacier at the confluence of the rivers Norte and Bayo (Fig. 2B), suggesting that ice was still present in this area at least until 10 ka (Glasser *et al*., 2012).

Thorndycraft *et al*. (2019) propose a model for the evolution of the glaciers and lakes at this latitude. In their model, they reinterpret the two ^{10}Be

exposure ages obtained by Glasser *et al*. (2012) as the minimum opening age of proglacial Chelenko Lake via the BRV. However, Bourgois *et al*. (2019) note that they do not consider the younger OSL age (9.7 ka) published by Glasser *et al*. (2012) which, in their interpretation, implies that the valley was still covered by glaciers 10 ka ago. They conclude that this valley never drained the Chelenko Lake.

The controversy concerning the hydroclimatic evolution of the area, therefore, focuses on the small number of available glaciation-related ages in the BRV. On the one hand, a single OSL age supports a late opening of the BRV. In fact, here is considerable scatter of OSL ages around the GCBAL basin and to base an interpretation on a single OSL is not recommended (*e.g.*, Thomsen *et al*., 2005). On the other hand, two ages deduced from ^{10}Be concentrations in erratic boulders suggest an early opening of the valley compatible with the model presented by Thorndycraft *et al*. (2019). However, ages deduced from erratic boulder must be considered with care due to inherited exposure history of the boulder: they may be underestimated if the boulders remained buried before being deposited and, instead, overestimated in case the boulder had accumulated cosmogenic isotopes before its final emplacement.

In the following, we will present new ^{10}Be concentrations directly from bedrock surfaces of the BRV that have been moulded by glacial erosion, which further diminishes the possibility of inherited cosmogenic isotope concentration and thus overestimation of exposure ages.

3. Methodology

3.1. Geomorphological maps and profiles

The identification and mapping of the different landforms of the BRV was carried out in the field and using satellite imagery from different sources, including Bing, ESRI and Google Earth. The topography analysis was developed based on an ALOS PALSAR digital elevation model (DEM) with a cell size of 12.5 m. Altitude was corrected with GeoidEval resulting vertical accuracy and precision of ~5 m. It is possible to identify the landform limits in vegetated covered areas by slope changes, so a DEM-based slope map was generated. The classification, general definition and identification criteria of the different landforms are presented in Table 1. Approaches and frameworks used agree with the revision of Chandler *et al*. (2018).

The identified landforms were further classified according to their altitude (±5 m) on a thalweg profile. The corrected DEM was used to generate this profile and to obtain the altitude and position of landforms. In the case of hanging valleys, the altitude considered corresponds to their minimum altitudes over the knickpoint; for glacial cirques, the considered altitude is that of their flat bottom; and for the rest of the landforms, the maximum, minimum and average altitudes were obtained. Transverse profiles were generated to show the relationship of some landforms in cross-valley sections.

3.2. Sampling of ice-moulded surfaces

Three ice-moulded surface samples with glacial striations on the valley floor were collected at a depth of 1-2 cm (sample thickness) for subsequent dating by ^{10}Be concentrations in quartz (Figs. 2 and 3). An analysis of cosmogenic nuclides on the hard rock ice-moulded surface may provide information on the timing of glacial retreat rates. This requires that a minimum thickness of three meters of rock has been removed by glacial erosion so that there is no inherited cosmogenic nuclide in the rock before glacial retreat (Ivy-Ochs and Kober, 2008). This condition would be fully met, given the magnitude of glacial erosion in the Patagonian Cordillera, which has been able to excavate several tens of meters of rock substrate during the glacial advance related to LLGM (Davies *et al*., 2020). Then, cosmogenic concentrations in ice-moulded bedrock surfaces give minimum age for glacial retreat. The topographic shielding was taken into account for the age calculation.

3.3. Cosmogenic ^{10}Be exposure ages

All samples were chemically performed at *Laboratoire National des Nucléides Cosmogéniques* (LN2C) at CEREGE (Aix en Provence, France) and targets of purified BeO were prepared for AMS measurement at *ASTER, the French National AMS Facility* (CEREGE, Aix en Provence). The measurements were calibrated against an In-House standard (STD11) NIMB of Braucher *et al*. (2015), using an assigned ^{10}Be/^{9}Be ratio of $(1.191)\times10^{-11}$ (1.09%). Analytical uncertainties (reported as 1σ) included for all samples the counting statistics,

TABLE 1. SUMMARY OF GLACIAL AND PARAGLACIAL LANDFORMS, MAPPING CRITERIA AND IMPLICATIONS OF THE PRESENCE OF EACH LANDFORM.

	Mapping Criteria			Implications	
Landform	**Morphology**	**Identification criteria**	**Uncertainty**	**Interpretation**	**Observations/Limitations**
Glacial abrasion surface 	Generally elongated low-relief surfaces	Elevated terrace-like surfaces usually disposed on the valley slopes, with signs of glacial erosion and slopes of 0-5° perpendicular to the valley direction	Its formation can be attributed to structural features of the bedrock. Potential confusion with outwash plains hanging in low-relief surfaces	Glacial erosion marks created during its drift. Can delimit the elevation at the base of the former glacier and minimum of its upper surface	Classified in low, medium and great altitude abrasion surfaces according to their distribution in the valley
Glacial ridge 	Generally elongated positive-relief ridges	Ridges with dark/light shading on opposing sides in aerial imagery, indicating a positive-relief hill. Breaks on the slope in DEM. Association with glacial abrasion surfaces	Potential overestimation of the relief and confusion with landforms generated by water-flow erosion after glacier drift	Rock eroded by glaciers with greater resistance to erosion than rock surrounding it, probably because of lithology and structural features	In this study was not possible to identify paleo-ice-flow directions, due to DEM's low resolution. Field description of this landforms is suggested
Terminal moraine 	Linear to arcuate positive-relief ridges. Usually perpendicular to valley	Ridges with dark/light shading on opposing sides in aerial imagery, indicating a positive-relief hill. Generally located in the terminal margins of a glacier, perpendicular to the valley. Visible break on slope of internal side of the arc	Potential confusion with mass wasting deposits due to vegetation covering	Till accumulated on the glacier front during its retreat. Marks a position of maximum glacier advance not erased by subsequent advances	Hierarchically classified according to position in relation to the valley in where they were formed. A greater number indicates an older and farther moraine front for the respective valley/glacier
Lateral moraine 	Elongated positive-relief ridges	Ridges found on the rock walls of a glacial valley. Low-inclination upper face usually covered by dense vegetation, with a break of slope in DEM. Generally found on steep walls without vegetation covering, of grey color, and coarse-grained texture. Usually shaded in satellite imagery	Potential confusion with colluviums or rock slopes when break on slope is absent and/or deposits are low in size. Potential confusion with eskers o ice-contact landforms when present similar morphologies and dispositions, and when covered by dense vegetation	Till mixed with sediment derived from valley walls or colluviums on the margins of a glacier during its advance	Size can vary depending on the criteria used to separate a terminal from a lateral moraine for a respective moraine front. Generally unstable, so may be overprinted by colluviums grading form this landform
Elevated alluvial fan 	Fan-shaped landforms (or relict of one)	Relicts of former elevated fans, with marks of surface runoff. Generally found at the margin of active alluvial fans. Recognized by a clear shading in satellite imagery, indicative of a scarp or steep slope and its elevated characteristic	Generally surrounded by bedrock with extensive vegetation covering, so extension of landform may be not precisely delimited. High inclination when found at the junctions of little basins with the main valley, so may be misinterpreted as colluvium. As no stratigraphic study is presented a formation on the margins of paraglacial lakes cannot be confirmed	Potential formation on the margins of a water body that stabilized its level on a higher elevation than present lakes	Hierarchically classified according to elevation. Field characterization of this deposits is suggested in order to corroborate its origin on the margins of a water body

continue table 1.

	Mapping Criteria			Implications	
Landform	**Morphology**	**Identification criteria**	**Uncertainty**	**Interpretation**	**Observations/Limitations**
Active alluvial fan 	Fan-shaped landforms	Found at the confluence of tributary basins and the main valley. Convex shape on transverse profile and concave shape on longitudinal profile. Slopes of 5-10° in wide sections and 10-15° in narrow sections of the valley	Potential confusion with floodplain when inclinations are low (<5°). Potential misclassification as colluviums when of high inclination (>15°), little extension and covered by vegetation	Indicative of water flowing from a tributary towards the main valley	Included in map as an "active cone-shaped landform"
Active fan delta 	Fan-shaped or cone-shaped landforms	Slopes of 0-5°. Found at the mouth of a river where it debouches into a larger body of water (lake, ocean). Dark brown color and signs of water flow	Difficult to delimitate when associated with a broad active floodplain, so actual size may be overestimate/underestimated	Indicative of a river flowing into a bigger water body	Size and slope may be indicative of sedimentation rates and accommodation space. Included in map as an "active cone-shaped landform"
Colluvium 	Fan-shaped or cone-shaped landforms	Slopes of 30° or more in DEM. Generally grey and no signs of water flow marks in satellite imagery. Usually surrounded by high-inclination terrain	Potential confusion with alluvial fans in narrow valleys or mass wasting deposits when dense vegetation cover is present. Potential confusion with moraine scarps when no break in slope is present in DEM nor shading in satellite imagery	Accumulation of material at the base of hillslopes primarily by gravity. Indicates a lesser influence of water flow on deposition	Included in map as an "active cone-shaped landform"
Mass wasting scarp and deposit 	Prominent breaks on the slope originating a steeped topography, semicircular scarps, and irregular deposits with signs of downslope flow	Irregular deposits that generate a positive relief in DEM. Association with a semicircular scarp and depressed topography, generating a notorious local increase in slope in DEM; color change and vegetation cover in satellite imagery	Potential misinterpretation as moraines when have irregular shapes. Scarp is often not clear in satellite imagery and DEM	Indicative of unstable rock slopes and adjustment to deglaciated conditions	Size limited to ~0.5-1 km, so lower scale mass wasting deposits are not considered, such as rockfalls, debris flows, snow avalanches, among others
Active floodplain 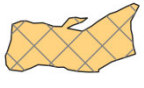	Approximately flat and regular surface covering the valley floor	Approximately flat surface (<1°). Laterally delimited by rock slopes and deposits, that increase inclination on DEM. Imprinted by abandoned meander channels and vegetation covering that follow fluvial patterns	Potential confusion with other low-slope landforms such as alluvial fans, fan deltas, and outwash plains, leading to an overestimation/underestimation of its actual size	Indicative of low-energy water flows from lakes, glaciers, and surface runoff	The low inclination enhances a lateral migration or rivers, and river patterns can shift rapidly when affected by external factor, such as heavy rains or rain deficits
Outwash plain 	Undulating and low-relief surface grading from ice-margin features	Low-inclination surface (1-3°). Brown-to-grey color and coarse-grained texture. Imprinted by water flow marks left by braided rivers grading from proglacial lakes or melting of glaciers	Coarse-grained texture often not recognizable in satellite imagery. Potential confusion with active floodplain when covered by vegetation	Indicative of meltwater flows	

the machine stability for the batch and an external uncertainty of 0.5% (Arnold *et al.*, 2010). The ^{10}Be half-life of (1.387±0.01)×10^{6} years (Chmeleff *et al*., 2010) was used.

Cosmogenic ^{10}Be exposure ages were calculated using the online CREp calculator (crep.crpg.cnrs-nancy.fr; Martin *et al*., 2017). They were computed using the scaling scheme Lal/Stone time dependent (Balco *et al*., 2008; Lal, 1991; Stone, 2000), with the ERA-40 (Uppala *et al*., 2005), the geomagnetic record of Atmospheric ^{10}Be-based VDM (Muscheler, *et al*., 2005; Valet *et al*., 2005) and the production rates (4.03±0.16 at/gr/yr) calibrated by Kaplan *et al*. (2011).

Calculation of topographic shielding was included considering the fieldwork observations. Age calculations consider an erosion rate of 0 mm/ka, as the percentage of variation per mm of erosion is only 1%, significantly less than the error associated with the ^{10}Be measurement. Additionally, the ^{10}Be exposure ages obtained by Glasser *et al*. (2006) in the Tranquilo River valley were recalculated using the same calculator.

3.4. Radiocarbon ages

Aniya *et al*. (2007) radiocarbon ages for wood, plants, and organic matters were calibrated and converted to calendar years BP using the OxCal 4.4 program with the SHCal20 terrestrial calibration curve for the southern hemisphere (Hogg *et al*., 2020) and are presented with a 2σ confidence interval (95.4% of the distribution probability). Ages >300 years are presented with the median values resulting from this calibration (Fig. 3B).

4. Results

4.1. Geomorphological mapping

The BRV presents characteristics of a paraglacial environment: fluvial-lacustrine processes and the adjustment of the slopes following glacial retreat have partially modified a valley previously carved by the glacier tongue coming from the core of the Patagonian Cordillera. For the identification and description of the landforms (Table 1), we used a geomorphological map together with a longitudinal profile of the thalweg and cross-valley profiles. The geomorphological map allows the identification of landforms with different origins (Figs. 2 and 3). The longitudinal thalweg profile includes the average height of the most relevant landforms (Fig. 4). The transverse profiles of the valley also include the position of the landforms described in the geomorphological map (Fig. 5).

In terms of glacial geomorphology, no significant moraine was identified in the valley floor upstream of KP2, whereas downstream lateral and frontal moraines are present (Figs. 2 and 3). Ice-moulded surfaces are observed on the slopes and valley bottom of the Tranquilo River Valley (Profile 1 in figure 5) and in the eastern segment of the BRV. These surfaces correspond to landforms generated by glacial erosion at different altitudes. To the West, the notable increase in the area covered by vegetation makes it difficult to identify ice-moulded surfaces on the slopes, which is why they were not recognized and mapped.

Alluvial fans coming from lateral valleys are preserved in the eastern sector, above the Tranquilo Valley and the Bayo Pass. Some alluvial fans (Al2) hanging between 450 and 550 m a.s.l. are preserved above the Bayo Pass (Fig. 4). Most fans along the Tranquilo Valley emplaced at a similar altitude of approximately 350 m a.s.l. (Al1 in figures 2B and 4). Alluvial fans are absent to the west, where the valley is more incised and a canyon morphology is accompanied by landslide scarps and glacial truncated spurs. In this area, landslide deposits are present in at least three sectors (Fig. 3A). The top of the eastern landslide deposit is located 40-50 m above the thalweg (Profile 2 in figure 5), at an elevation similar to the lowest alluvial fans observed east of Bayo Pass (350 m a.s.l.).

The Exploradores is an active glacier that originates in the northeastern flank of Mount San Valentín and descends northward towards the Exploradores River Valley (Fig. 2A). The front of the glacier is marked by the presence of two terminal moraines (TM1 and TM2; Fig. 3B) (Aniya *et al*., 2007). Another terminal moraine (TM3) is located 3 km downstream, where it is adjacent to a mass wasting deposit (see Profile 3 in figure 5). The main moraine (TM2) is the most prominent and conforms a 150 m-high ridge above the valley floor. This morainic ridge located close to the confluence of the Exploradores and Bayo Rivers causes the presence of KP3.

Radiocarbon ages from frontal moraines of the Exploradores Glacier (Aniya *et al*., 2007) record

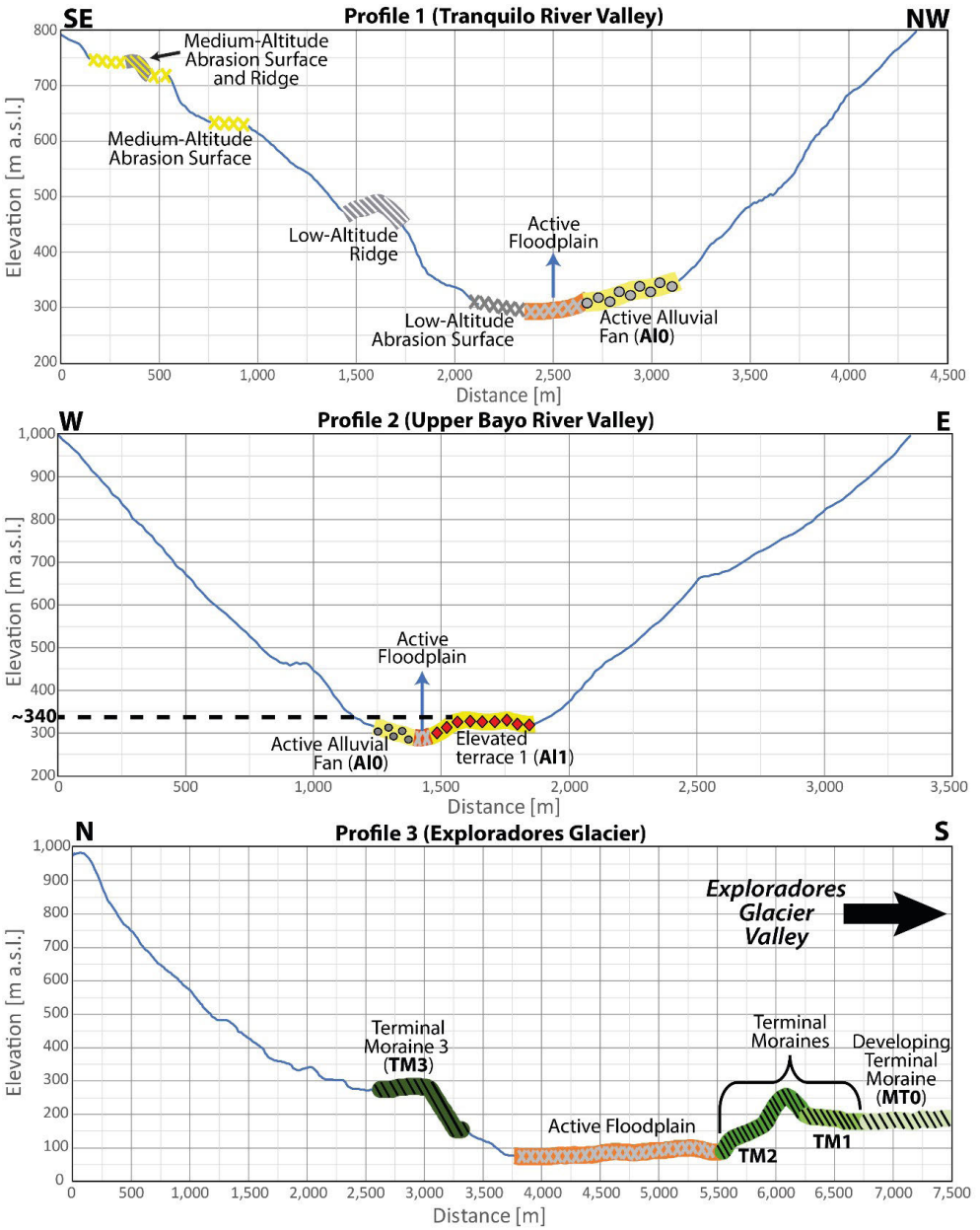

FIG. 5. Cross-sectional profiles (see location in Figs. 2 and 3).

only recent (<1.79 cal. ka BP) glacial and paraglacial dynamics (Fig. 3B). A single older age of ~10.4 cal. ka BP has been obtained for the main frontal moraine (TM2; Fig. 3B). This age indicates that the ice must have retreated from that part of the valley to allow its colonization by vegetation. However, considering the several younger ages obtained in this moraine, this old age is likely to date an ancient organic material reworked by younger moraines (Aniya *et al*., 2007).

4.2. Cosmogenic ^{10}Be exposure ages

Samples were collected on ice-moulded surfaces close to the floor of the BRV (location on figures 2

and 3). Samples BA-1 and BA-2 were collected close to the Bayo Lake (Fig. 6). BA-1 and BA-2 were collected at altitudes of 139 and 131 m a.s.l., respectively, *i.e.*, a few meters above the Bayo Lake whose present-day level is 124 m a.s.l. (Fig. 4). In the upper BRV, BA-4 was sampled a few km downstream of Bayo Pass (Fig. 6), at 341 m a.s.l. Table 2 shows measured cosmogenic ^{10}Be concentrations and calculated exposure ages. This table also includes the recalibrated ages calculated for the samples presented in Glasser *et al*. (2006).

BA-1 and BA-2 (14.05±0.94 ka and 14.55±1.8 ka, respectively; Table 2) are the first cosmogenic ages reported in the Bayo Lake area. The two sampling points are on steep ice-moulded surfaces at the foot of elevated slopes of a deeply incised glacial trough,

FIG. 6. Photographs of sampling areas. **A-B.** Location of sample BA-1. **C.** Sampling site BA-2. **D-E.** Sampling site of BA-4.

TABLE 2. SAMPLE INFORMATION, THE MEASURED ^{10}BE CONCENTRATIONS AND THE CALCULATED EXPOSURE AGES.

Sample ID	Latitude (°)	Longitude (°)	Altitude (m)	Sample thickness (cm)	Topographic Shielding[a]	^{10}Be concentrations[b] (at/gr^{-1})	Age[c] (Kyears)	Source of measure
BA-1	-46.49	-73.12	139	1.1	0.883	56,406±3,208	14.05±0.94	This work
BA-2	-46.50	-73.08	131	1.1	0.851	55,930±6,787	14.55±1.8	This work
BA-4	-46.63	-72.84	341	1.4	0.985	70,149±6,113	12.98±1.21	This work
LTE-1	-46.61	-72.76	336	3	0.991	77,100±4,700	14.4±1	Glasser *et al*., 2006
LTE-2	-46.61	-72.76	317	4	0.98	68,600±3,800	13.31±0.88	Glasser *et al*., 2006
LTW-1	-46.65	-72.81	773	3	0.982	120,000±4,500	15.42±0.8	Glasser *et al.,* 2006

[a] Correction factor calculated according to the shielding by the surrounding topography.
[b] Errors are at the 1σ level and include the AMS analytical uncertainties, including the error of the subtracted blank, and the uncertainly of production rates (Kaplan *et al*., 2011).
[c] Cosmogenic ^{10}Be exposure ages were calculated on Tue Aug 10 2021, using the online CREp calculator (crep.crpg.cnrs-nancy.fr; Martin *et al*., 2017). All samples considering quartz with a density of 2.5 g/cm^3.

explaining the significant topographic shielding that must be considered to evaluate the ages (Table 2). Fig. 7A shows the overlapped curves of probability ages of BA-1 and BA-2, where the 1σ intersect in a range between 13.1 ka and 15 ka.

BA-4 in the Bayo Pass area (Fig. 6) gives an age of 12.98±1.21 ka (Table 2), which is slightly younger than the two recalibrated ages of 13.31±0.88 ka and 14.4±1 ka obtained for the two erratic boulders sampled by Glasser *et al*. (2006) on the eastern shore of Tranquilo Lake (Fig. 2B). In fact, the uncertainty (1σ) of the age of BA-4 (11.77-14.19 ka; Fig. 7B) overlaps those of LTE2 (12.43-14.19 ka) and LTE1 (13.4-15.4 ka). Uncertainties intersect between 13.4 ka and 14.2 ka for these three samples.

Although ages obtained both, close to the Bayo Pass and those obtained close to the Bayo Lake, vary between each sample, they do not differ significantly: their 1-sigma uncertainty overlaps in the range between 13.4 ka and 14.2 ka (Fig. 7) evidencing that the set of processes that determined the ages obtained from the valley floor in both areas occurred over a similar time range. Finally, another boulder from a lateral moraine near an elevated cirque of a hanging tributary valley (LTW-1, 770 m a.s.l.; Table 2 and Fig. 2B) was dated by Glasser *et al*. (2006). Its recalibrated age is 15.42±0.8 ka, thus slightly older than the age range obtained in the valley floor.

5. Discussion

The age of 12.98±1.21 ka in ice-moulded surfaces in the valley floor of the Bayo Pass area (BA-4) is comparable to the two ages of erratic boulders (LTE2 of 13.31±0.88 ka and LTE1 of 14.4±1 ka) obtained by Glasser *et al.* (2006). If we consider an uncertainty of 1 sigma, these ages also overlap BA-1 and BA-2 ages (14.05±0.94 ka and 14.55±1.8 ka, respectively) obtained close to the Bayo Lake (Fig. 7). The age range that satisfies the 5-sample error overlap is 13.4-14.2 ka.

Cosmogenic concentrations in ice-moulded surfaces indicate minimum ages for the retreat of the glacier from the BRV. Indeed, in basement rocks, pre-glacier inherited concentrations could only be preserved if less than a few meters of rocks were eroded during the glacial period, which seems unlikely given the several hundred meters-thick glacial tongue that flowed within the valley.

In contrast, several processes may have protected ice-moulded surfaces from cosmogenic radiations following the retreat of ice: a soil or sediment layers may have temporarily covered the bedrock. This possibility may be considered for the BA-4 sample that has been collected on a roughly horizontal surface. It is unlikely for BA-1 and BA-2 that correspond to steeply inclined surfaces (see Fig. 7). Moreover, Thorndycraft *et al*. (2019) also note that exposure

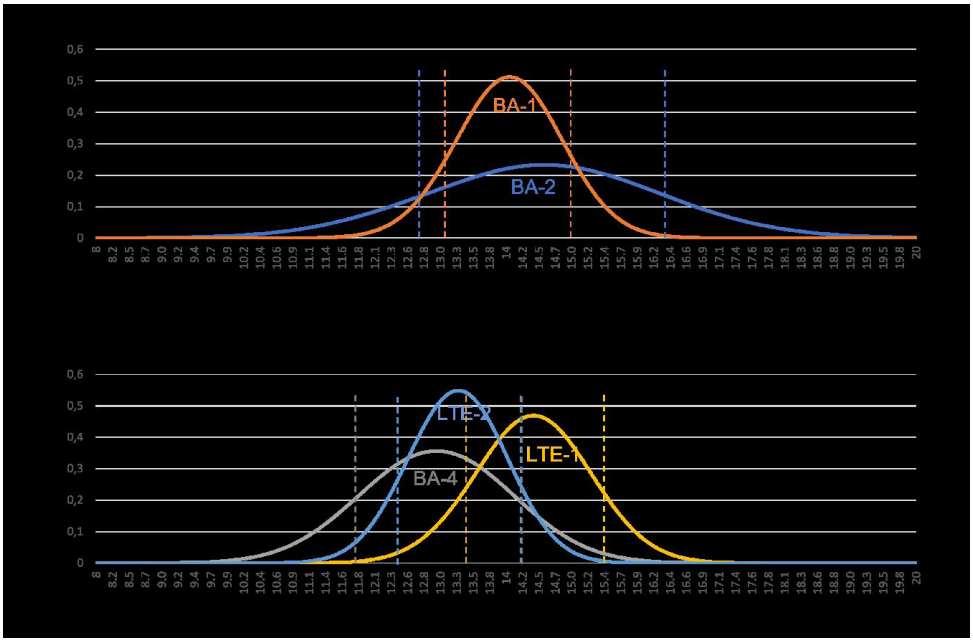

FIG. 7. Probability density function curves calculated from the exposure ages. Age of samples BA1, BA2 and BA4 obtained in this work and LT-1 and LT-2 recalibrated from data of Glasser *et al*. (2006). Segmented line shows 1 sigma uncertainty. A: samples in Bayo Lake area. Their 1-sigma uncertainty overlaps in the range between 13.1 ka and 15 ka. B. samples in Bayo Pass area. Their 1-sigma uncertainty overlaps in the range between 13.4 ka and 14.2 ka.

ages post-date ice-retreat if the rock was covered by a pro-glacial lake. Ages indicate instead the moment when samples emerge following the lowering of the lake level.

The altitude of the mapped alluvial fans (Al2 and Al1) in the Tranquilo Valley and Bayo Pass coincides with the altitude of the lake terraces of the GCBAL (T2 and T1). We interpret these alluvial fans to be remnants of lake levels which can be correlated with the ancient lake levels of the GCBAL (Deseado and Chelenko). The Al2 alluvial fan present above the Bayo Pass at ~460 m a.s.l. shows that BA-4 sample remained more than one hundred meters beneath the level of a lake following the retreat of the glacier. The altitude of this lake is that of the Deseado Lake, whose outlet was toward the Atlantic Ocean (*e.g*., Thorndycraft *et al*., 2019). Hence, ^{10}Be exposure age of BA-4 does not date the retreat of the glacier from the Bayo pass, but instead the subsequent lowering of the lake level from Deseado to Chelenko lakes, and glacial retreat must have occurred prior to its exposure age. This agrees with the age obtained in moraines associated to glacial advance in the hanging tributary valley of 15.42±0.8 ka at an altitude of 770 m a.s.l. by Glasser *et al*. (2006) because their preservation is only possible if the trunk valley is uncovered by ice.

Figure 8 shows a conceptual model of the evolution of glacial cover in the BRV. Initially, the valley was covered by the glacier that dammed the outlet of Deseado Lake (Fig. 8A). During this stage, the T2 terraces observed all around the GCBAL (Martinod *et al*., 2016) formed. They correlate with the alluvial level Al2 identified in the Bayo Pass. After the glacier retreated from the BRV, the valley was able to drain the lake, thus lowering its level. When the level stabilized, Chelenko Lake was formed (Fig. 8B). During the Chelenko stage, the T1 terraces formed all around the lake. They correlate with the alluvial level Al1 identified in the Tranquilo Valley. The lake abandoned the Tranquilo Valley following the opening of the Baker River Valley (Fig. 8C). Different authors describe the formation of this large lake connecting the GCBAL and Cochrane-Pueyrredón Lakes, whose level stabilizes around 350 m a.s.l. before the opening of the Baker River Valley (Turner *et al*., 2005; Bell, 2008; Glasser *et al*., 2016; Hein *et al*., 2010; Martinod *et al*., 2016; Thorndycraft *et al*., 2019; Isla and Espinosa, 2021).

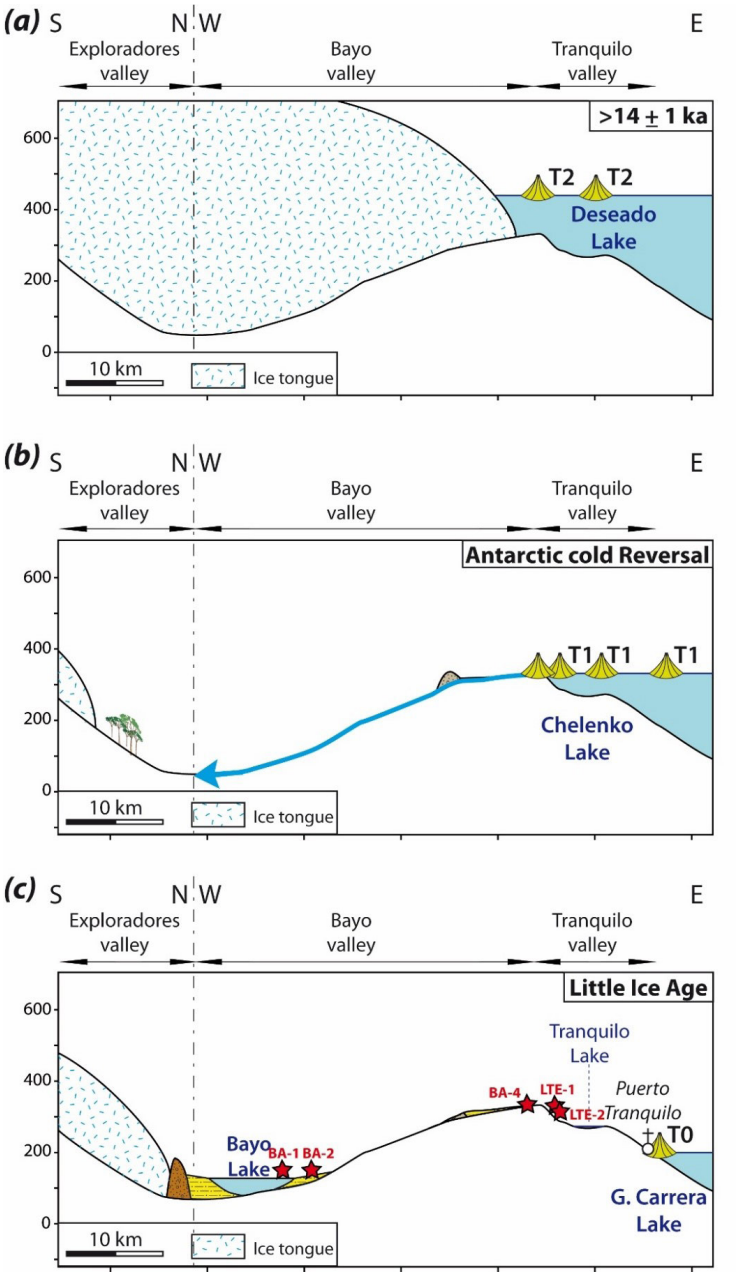

FIG. 8. Conceptual model of the evolution of the BRV in relation to the ice and lake extends. **T0:** Recent lake-terraces (210 m a.s.l.). **T1:** Chalenko lake-terraces (~350 m a.s.l.). **T2:** Deseado lake-terraces (~460 m a.s.l.). Red starts show sites of ^{10}Be cosmogenic exposure ages.

Certainly, an age of deglaciation before 13.4-14.2 ka is not in agreement with a glacial advance through the BRV that would have reached the Bayo Pass at 10 ka, as proposed by Glasser *et al.* (2012). In fact, the cosmogenic isotopes concentrations do not formally mean that there was no glacial re-advance in the valley, *e.g.*, around 10 ka as suggested by the OSL age of 9.7 ka in glacio-fluvial deposits in the Bayo Pass: they could have been modest advances that did not erode the pre-existing ice-moulded surfaces.

However, ^{10}Be concentrations indicate that the valley floor was not eroded by glaciers after 13.4-14.2 ka both close to the Bayo Pass (BA-4 sample) and close to the Bayo Lake (BA-1 and BA-2 samples). The Bayo Lake is located ~40 km west of the Bayo Pass. If a major advanced had taken place in the valley after 13.4-14.2 ka, a 40 km-long glacial tongue originating from the Exploradores Valley and flowing eastward in the valley toward the Bayo Pass would have eroded again the lake area and diminished the amount of inherited cosmogenic isotopes in BA-1 and BA-2, which is not observed.

Cosmogenic isotope concentrations indicate the minimum age of glacial retreat from the BRV, we therefore conclude that the valley was free of ice at 13.4-14.2 ka ago. This age, indicated by the BA-1 sample, agrees with BA-2. The exposure age of BA-4 is slightly (although not significantly) younger, which may suggest a minor erosion of the ice-moulded surface and/or a temporary covering of the sampled bedrock. This early retreat of the glacier from the BRV confirms that this valley constituted the outlet of the Chelenko lake to the Pacific Ocean at the end of the Pleistocene before the opening of the present-day Baker Valley that drained the GCBAL in the Holocene; *i.e.,* the BRV drained the lake when the Baker valley was still closed by ice during the Antarctic Cold Reversal. The timing of this early outlet of the GCBAL to the Pacific Ocean is close to the timing of Atlantic/Pacific drainage reversal in Palena sector at 16 ka (43º S; Leger *et al*., 2021).

In the Bayo Lake sector, the valley exhibits a flat topography, covered by fluvio-lacustrine sediments, that filled this over-deepened section of the valley (Fig. 8C). It should be noted that samples BA-1 and BA-2 were collected only a few meters above the current Bayo Lake level. Then, their cosmogenic ages indicate that the level of this lake has never been higher than today following the retreat of the glacier from the valley. This is confirmed by the absence of preserved terraces around the lake. This lake results from the presence of the main terminal moraine of Exploradores Glacier (TM2), which partially dams the outlet of the Bayo valley (Fig. 3B).

The wonderful moraine preservation of Exploradores Glacier clearly shows it constituted the terminal moraine of a glacier until recently. This is confirmed by radiocarbon ages obtained in this moraine by Aniya *et al*. (2007). These authors conclude that both TM2 and TM3 formed during the Little Ice Age, TM2 before the 17th century and TM3 during the 19th century. A single old radiocarbon age (~10.4 cal. ka BP) has been obtained by Aniya *et al*. (2007) in TM2. This older radiocarbon age dates a reworked organic material carried downwards by the glacier, rather than a vegetation growth in the moraine following colonization. This age confirms that the retreat of the glacier from the Bayo Valley was rapid and occurred before ~10.4 ka BP, and the glacial edge of Exploradores Glacier was located at the same position or upstream TM2 to permit the growth of vegetation. The new advance of the glacier during the Little Ice Age carried the woods that had grown upstream in the Exploradores valley, and built a moraine (TM2) that partially dammed the Bayo River outlet, creating the Bayo Lake. The Bayo Lake is therefore a very recent feature whose elevation has been controlled by the Little Ice Age advance of Exploradores Glacier. Studying the sediment in this lake would give direct information on the recent dynamics of the glacier.

We conclude that BRV was glacially uncovered prior to 13.4-14.2 ka and that it is possible that exposure ages are controlled partly by paraglacial processes occurring after the complete deglaciation of the valley, including the presence of lakes that covered the glacial deposits and erosion features. After the LLGM, glacial advances in Patagonia are usually assigned to wet and cold periods that occurred at the end of the late Pleistocene linked to the Heinrich Stadial 1 (HS1; 18-14.5 ka; Rasmussen *et al*., 2006), the Antarctic Cold Reversal (ACR; 14.5-12.9 ka; Jouzel *et al*., 2001) and the Younger Dryas (YD; 12.9-11.7 ka; Rasmussen *et al*., 2006). Nevertheless, our results indicate that during these two more recent periods (ACR and YD) the BRV valley-floor remained ice-free and that a glacier occupied the valley only during HS1. The HS1 period corresponds to the Deseado lacustrine stage during which the precursor of the General Carrera Lake flowed towards the Atlantic via the Deseado valley. The corresponding lake level at >400 m a.s.l. is confirmed by terraces produced by fan deltas that formed before 15 ka according to Thorndycraft *et al*. (2019). This age agrees with the minimum age of 13.4-14.2 ka we deduce from cosmogenic concentrations, confirming that the Bayo Valley constituted the first possible outlet of the lake toward the Pacific Ocean following the end of the LLGM. The opening of the BRV agrees with the lake-level

drop from 470-400 m a.s.l. (Deseado level) to 360-300 m a.s.l. (Chelenko level) around 14.8 ka according to radiocarbon dates from lake sediment cores and new OSL dating (Vásquez *et al*., 2022).

Following the opening of the BRV before 13.4-14.2 ka, glacier retreated upstream of the confluence between the valleys of Exploradores and Bayo Rivers. The presence of a radiocarbon age of ~10.4 cal. ka BP in the TM2 terminal moraine (Aniya *et al*., 2007) of the Exploradores Glacier suggests that the maximum advance of the glacier during the last 10 ka occurred at similar or upper position that the glacial stage occurred during the Little Ice Age. The fluctuations of Ventisquero Exploradores are therefore comparable to those described for other glaciers in Patagonia and Tierra del Fuego such as the Marinelli Glacier, whose main advance since its rapid retreat 15 ka ago occurred during the Little Ice Age, 5 centuries ago (Hall *et al*., 2019).

6. Conclusions

We propose that the Late Pleistocene and Holocene evolution of the Bayo River Valley has been largely controlled by the retreat of the Northern Patagonian Ice Field. Fig. 8 summarizes the evolution of the valley, initially filled by a glacial tongue originating from the core of the Patagonian Cordillera that separated in two divergent glaciers: the western one flowed toward the Pacific Ocean and the eastern glacier tongue overlaid the Bayo Pass and flowed toward the future GCBAL. Following the end of LLGM, the icecap retreated and the precursor of GCBAL (Deseado Lake), whose elevation was ~400 to 450 m a.s.l., flowed to the Atlantic Ocean. The cosmogenic nuclide concentrations in the Bayo Valley indicate that the valley floor was ice-free at 13.4-14.2 ka ago. Because the valley was deglaciated, Chelenko Lake could be drained into the Pacific Ocean via the BRV before the activation of the drainage via the Baker River. We thus conclude that it is not necessary to invoke any endorheic stage to explain the successive elevation of paleo-shorelines observed around the GCBAL. Perito Moreno pass elevation, at the eastern end of GCBAL, controlled the Deseado Lake level, and the elevation of the Bayo Pass controlled the level of the lake during the following Chelenko stage. The cosmogenic nuclide concentrations also suggest that the Little Ice Age glacial advance of Exploradores Glacier has been the largest one during the last 13.4-14.2 ka, and that its frontal moraine controlled the present-day level of the Bayo Lake.

Acknowledgments

G. Aguilar and M. Gallardo were supported by the Advanced Mining Technology Center (AMTC) financed by ANID Project AFB180004. J. Martinod and C. Sue acknowledge financial support by the INSU-Syster program. We thank V. Flores-Aqueveque and E. Sagredo for contributing with the undergraduate thesis of M. Gallardo. This text was improved thanks to the comments and revision of Dr. V. Thorndycraft and the editor Dr. W. Vivallo.

Particular thanks are due in this paper to D.L. Bourlès† of the ASTER team, who in his lifetime (1955-2021) was involved in numerous contributions to various applications of cosmogenic nuclides in Andean geology (Braucher *et al*., 2021). The ASTER AMS national facility (CEREGE, Aix-en-Provence, France) is supported by the INSU/CNRS, the ANR through the "Projets thématiques d'excellence" program for the "Equipements d'excellence" ASTER-CEREGE action and IRD. AsterTeam (D. Bourlès, R. Braucher, G. Aumaître, K. Keddadouche) are warmly thanked for their expertise in AMS.

References

Aniya, M.; Enomoto, H.; Aoki, T.; Matsumoto, T.; Skvarca, P.; Barcaza, G.; Suzuki, R.; Sawagaki, T.; Sato, N.; Isenko, E.; Iwasaki, S.; Sala, H.; Fukuda, A.; Satow, K.; Naruse, R. 2007. Glaciological and geomorphological studies at Glaciar Exploradores, Hielo Patagonico Norte, and Glaciar Perito Moreno, Hielo Patagonico Sur, South America, during, 2003-2005(GRPP03-05). Bulletin of Glaciological Research 24: 95-107.

Arnold, M.; Merchel, S.; Bourlès, D.; Braucher, R.; Benedetti, L.; Finkel, R.; Aumaître, G.; Gottdang, A.; Klein, M. 2010. The French accelerator mass spectrometry facility ASTER: Improved performance and developments. Nuclear Instruments and Methods in Physics Research, Section B: Beam Interactions with Materials and Atoms 268 (11-12): 1954-1959.

Balco, G.; Stone, J.O.; Lifton, N.A.; Dunai, T.J. 2008. A complete and easily accessible means of calculating surface exposure ages or erosion rates from ^{10}Be and ^{26}Al measurements. Quaternary Geochronology 3: 174-195.

Bell, C.M. 2008. Punctuated drainage of an ice-dammed Quaternary lake in southern South America. Geografiska Annaler, Series A: Physical Geography 90 A(1): 1-17. doi: https://doi.org/10.1111/j.1468-0459.2008.00330.x

Bendle, J.M.; Palmer, A.P.; Thorndycraft, V.R.; Matthews, I.P. 2017a. High-resolution chronology for deglaciation of the Patagonian Ice Sheet at Lago Buenos Aires (46.5 S) revealed through varve chronology and Bayesian age modelling. Quaternary Science Reviews 177: 314-339.

Bendle, J.M; Thorndycraft, V.R.; Palmer, A.P. 2017b. The glacial geomorphology of the Lago Buenos Aires and Lago Pueyrredón ice lobes of central Patagonia, Journal of Maps 13 (2): 654-673. doi: https://doi.org /10.1080/17445647.2017.1351908.

Bennett, M.M.; Glasser, N.F. 2011. Glacial geology: ice sheets and landforms. John Wiley & Sons: 400 p. London.

Boex, J.; Fogwill, C.; Harrison, S.; Glasser, N.F.; Hein, A.; Schnabel, C.; Xu, S. 2013. Rapid thinning of the late Pleistocene Patagonian Ice Sheet followed migration of the Southern Westerlies. Scientific Reports 3: 1-6. doi: https://doi.org/10.1038/srep02118

Bourgois, J.; Cisternas, M.E.; Braucher, R.; Bourlès, D.; Frutos, J. 2016a. Geomorphic records along the General Carrera (Chile)-Buenos Aires (Argentina) glacial lake (46o-48oS), climate inferences, and glacial rebound for the past 7-9 ka. Journal of Geology 124 (1): 27-53. doi: https://doi.org/10.1086/684252

Bourgois, J.; Cisternas, M.E.; Braucher, R.; Bourlès, D.; Frutos, J. 2016b. Geomorphic records along the general carrera (Chile)-buenos aires (argentina) glacial lake (46°-48°S), climate inferences, and glacial rebound for the past 7-9 ka: A reply. Journal of Geology 124 (5): 637-642. doi: https://doi.org/10.1086/687551

Bourgois, J.; Cisternas, M.E.; Frutos, J. 2019. Comments on: "Glacial lake evolution and Atlantic-Pacific drainage reversals during deglaciation of the Patagonia ice sheet" by Thorndycraft *et al*. (Quaternary Science Reviews 203 (2019), 102-127). Quaternary Science Reviews 213: 167-170. doi: https://doi.org/10.1016/j.quascirev.2019.03.036

Braucher, R.; Guillou, V.; Bourles, D.J.; Arnold, M.; Aumaître, G.; Keddadouche, K.; Nottoliet, E. 2015. Preparation of ASTER in-house $^{10}Be/^{9}Be$ standard solutions. Nuclear Instruments and Methods in Physics Research 361: 335-340.

Braucher, R.; Blard, P.H.; Brown, E.T.; Carcaillet, J.; Lebatard, A.E.; Siame, L.; Simon, Q.; Thouveny, N.; Aumaître, G.; Bard, E.; Carretier, S.; Cornu, S.; Fink, D.; Finkel, R.; German, CH.; Godard, V.; Gosse, J.; Hamelin B.; Hofmann, F.M.; Jomelli, V.; Keddadouche, K.; Kurz, M.D.; Matmon, A.; Palacios, D.; Measures, CH.; Merchel, S.; Regard, V.; Schimmelpfennig, I.; Von Blanckenburg, F.; Zerathe, S. 2021. Didier L. Bourlès (1955-2021), the 5 MV cosmogenic rock star. Quaternary Geochronology 65: 101186. doi: https://doi.org/10.1016/j.quageo.2021.101186

Caldenius, C.C.Z. 1932. Las Glaciaciones Cuaternarias en la Patagonia y Tierra del Fuego: Una investigación regional, estratigráfica y geocronológica. Una comparación con la escala geocronológica sueca. Geografiska Annaler, 14 (1-2): 1-164.

Chandler, B.M.P.; Lovell, H.; Boston, C.M.; Lukas, S.; Barr, I.D.; Benediktsson, I.O.; Benn, D.I.; Clark, C.D.; Darvill, C.M.; Evans, D.J.A.; Ewertowski, M.W.; Loibl, D.; Margold, M.; Otto, J.C.; Roberts, D.H.; Stokes, C.R.; Storrar, R.D.; Stroeven, A.P. 2018. Glacial geomorphological mapping: A review of approaches and frameworks for best practice. Earth-Science Reviews 185: 806-846. doi: https://doi.org/10.1016/j.earscirev.2018.07.015

Chmeleff, J.; Blanckenburg, F.; Kossert, K.; Jakob, D. 2010. Determination of the ^{10}Be half-life by multicollector ICP-MS and liquid scintillation counting. Nuclear Instruments and Methods in Physics Research Section B: Beam Interactions with Materials and Atoms 268 (2): 192-199.

Davies, B.; Thorndycraft, V.; Fabel, D.; Martin, J. 2018. Asynchronous glacier dynamics during the Antarctic Cold Reversal in central Patagonia. Quaternary Science Reviews 200: 287-312.

Davies, B.J.; Darvill, C.M.; Lovell, H.; Bendle, J.M.; Dowdeswell, J.A.; Fabel, D.; García, J.L.; Geiger, A.; Glasser, N.F.; Gheorghiu, D.M.; Harrison, S.; Hein, A.S.; Kaplan, M.R.; Martin, J.R.V.; Mendelova, M.; Palmer, A.; Pelto, P.; Rodés, A.; Sagredo, E.A.; Smedley, R.K.; Smellie, J.L.; Thorndycraft, V.R. 2020. The evolution of the Patagonian Ice Sheet from 35 ka to the present day (PATICE). Earth-Science Reviews 204: 103152. doi: https://doi.org/10.1016/j.earscirev.2020.103152

Douglass, D.; Singer, B.; Kaplan, M.; Michelson, D.; Caffee, M. 2006. Cosmogenic nuclide surface exposure dating on boulders on last-glacial and late glacial moraines and paleoclimatic implications. Quaternary Geochronology 1: 43-58.

Georgieva, V.; Melnick, D.; Schildgen, T.F.; Ehlers, T.A.; Lagabrielle, Y.; Enkelmann, E.; Strecker, M.R. 2016. Tectonic control on rock uplift, exhumation, and topography above an oceanic ridge collision: Southern Patagonian Andes (47°S), Chile. Tectonics 35 (6): 1317-1341. doi: https://doi.org/10.1002/2016TC004120

Glasser, N.F.; Harrison, S.; Ivy-Ochs, S.; Duller, G.A.; Kubik, P.W. 2006. Evidence from the Rio Bayo valley

on the extent of the North Patagonian Icefield during the Late Pleistocene-Holocene transition. Quaternary Research 65 (1): 70-77. doi: https://doi.org/10.1016/j.yqres .2005.09.002

Glasser, N.F.; Harrison, S.; Schnabel, C.; Fabel, D.; Jansson, K.N. 2012. Younger Dryas and early Holocene age glacier advances in Patagonia. Quaternary Science Reviews 58: 7-17. doi: https://doi.org/10.1016/j.quascirev.2012.10.011

Glasser, N.F.; Jansson, K.N.; Duller, G.A.; Singarayer, J.; Holloway, M.; Harrison, S. 2016. Glacial lake drainage in Patagonia (13-8 kyr) and response of the adjacent Pacific Ocean. Scientific Reports 6: 1-7. doi: https://doi.org/10.1038/srep21064

Hall, B.I.; Lowell, T.V.; Bromley, G.R.M.; Denton, G.H.; Putnam, A.E. 2019. Holocene glacier fluctuations on the northern flank of Cordillera Darwin, southernmost South American. Quaternary Science Reviews 222: 105904. doi: https://doi.org/10.1016/j.quascirev.2019.105904

Hein, A.S.; Hulton, N.R.J.; Dunai,T.J.; Sugden, D.E.; Kaplan, M.R. 2010. The chronology of the Last Glacial Maximum and deglacial events in central Argentine Patagonia. Quaternary Science Reviews 29: 1212-1227. doi: https://doi.org/10.1016/j.quascirev.2010.01.020

Hogg, A.G.; Heaton, T.J.; Hua, Q.; Palmer, J.G.; Turney, C.S.; Southon, J.; Bayliss, A.; Blackwell, P.G.; Boswijk, G.; Ramsey, C.B.; Pearson, C.; Petchey, F.; Reimer, P.; Reimer, R.; Wacker, L. 2020. SHCal20 Southern Hemisphere Calibration, 0-55,000 Years cal BP. Radiocarbon 62 (4): 759-778. doi: https://doi.org/10.1017/RDC.2020.59

Isla, F.I.; Espinosa, M. 2021. Quaternary glaciolacustrine deposits around a Triple Junction site: Paleolakes at the foot of the Northern Patagonian Ice field (Argentina and Chile). Andean Geology 48 (1): 94-109. doi: https://doi.org/10.5027/andgeoV48n1-3173

Ivy-Ochs, S.; Kober, F. 2008. Surface exposure dating with cosmogenic nuclides. E&G Quaternary Science Journal 57 (1/2): 179-209. doi: https://doi.org/10.3285/eg.57.1-2.7

Jouzel, J.; Masson, V.; Cattani, O.; Falourd, S.; Stievenard, M.; Stenni, B.; Longinelli, A.; Johnsen, S.J.; Steffenssen, J.P.; Petit, J.R.; Schwander, J.; Souchez, R.; Barkov, N.I. 2001. A new 27 ky high resolution East Antarctic climate record. Geophyscial Research Letters 28: 3199-3202.

Kaplan, M.R.; Ackert, R.; Singer, B.; Douglass, D.; Kurz, M. 2004. Cosmogenic nuclide chronology of millennial-scale glacial advances during the O-isotope stage 2 in Patagonia. Geological Society of America Bulletin 116: 308-321.

Kaplan, M.R.; Strelin, J.A.; Schaefer, J.M.; Denton, G.H.; Finkel, R.C.; Schwartz, R.; Putnam, A.E.; Vandergoes, M.J.; Goehring, B.M.; Travis, S.G. 2011. In-situ cosmogenic ^{10}Be production rate at Lago Argentino, Patagonia: Implications for late-glacial climate chronology. Earth and Planetary Science Letters 309 (1-2): 21-32. doi: https://doi.org/10.1016/j.epsl.2011.06.018

Lal, D. 1991. Cosmic ray labeling of erosion surfaces: in situ nuclide production rates and erosion models. Earth and Planetary Science Letters 104: 424-439.

Leger, T.P.M.; Hein, A.S.; Bingham, R.G.; Rodès, A.; Fabel, D.; Smedley, R.K. 2021. Geomorphology and ^{10}Be Chronology of the Last Glacial Maximum and deglaciation in north-eastern Patagonia, 43ºS-71ºW, Quaternary Sciences Reviews 272: 107194. doi: https://doi.org/10.1016/j.quascirev.2021.107194.

Martin, L.; Blard, P.-H.; Balco, G.; Lave, J.; Delunel,R.; Lifton, N.; Laurent, V. 2017. The CREp program and the ICE-D production rate calibration database: a fully parameterizable and updated online tool to compute cosmic-ray exposure ages. Quaternary Geochronology 38: 25-49. doi: https://doi.org/10.1016/j.quageo.2016.11.006

Martinod, J.; Pouyaud, B.; Carretier, S.; Guillaume, B.; Hérail, G. 2016. Discussion and reply geomorphic records along the General Carrera (Chile)-Buenos Aires (argentina) glacial lake (46°-48°S), climate inferences, and glacial rebound for the past 7-9 ka: A discussion. Journal of Geology 124 (5): 631-635. doi: https://doi.org/10.1086/687550

Mendelova, M.; Hein, A.; McCulloch, R.; Davies, B. 2017. The Last Glacial Maximum and deglaciation in central Patagonia, 44°S-49°S. Cuadernos de Investigación Geográfica 43 (2): 719. doi: https://doi.org/10.18172/cig.3263

Muscheler, R.; beer, J.; Kubik, P.W.; Synal, H.A. 2005. Geomagnetic field intensity during the last 60,000 years based on ^{10}Be and ^{36}Cl from the Summit ice cores and ^{14}C. Quaternary Science Reviews 24 (16-17): 1849-1860. doi: https://doi.org/10.1016/j.quascirev.2005.01.012

Munro-Stasiuk, M.J.; Heyman, J.; Harbor, J. 2013. Erosional Features. Treatise on Geomorphology 8: 83-99. doi: https://doi.org/10.1016/B978-0-12-374739-6.00197-4

Rabassa, J.; Clapperton, C.N. 1990. Quaternary Glaciations of the Southern Andes. Quaternary Science Review 9: 153-174. doi: https://doi.org/10.1016/0277-3791(90)90016-4

Rasmussen, S.O.; Andersen, K.K.; Svensson, A.; Steffensen, J.P.; Vinther, B.M.; Clausen, H.B.; Siggaard-Andersen,

M.L.; Johnsen, S.J.; Larsen, L.B.; DahlJensen, D. 2006. A new Greenland ice core chronology for the last glacial termination (1984e2012). Journal of Geophysical Research 111: 1-16.

Sernageomin. 2003. Mapa Geológico de Chile: Versión Digital. Base Geológica 1:1.000.000. Servicio Nacional de Geología y Minería, Chile. Publicación Geológica Digital No. 4, 2003.

Stone, J.O. 2000. Air pressure and cosmogenic isotope production. Journal of Geophysical Research 105: 23753. doi:https://doi.org/10.1029/2000JB900181

Thomsen, K.J.; Murray, A.S.; Bøtter-Jensen, L. 2005. Sources of variability in OSL dose measurements using single grains of quartz. Radiation Measurements 39: 47-61.

Thorndycraft, V.R.; Bendle, J.M.; Benito, G.; Davies, B. J.; Sancho, C.; Palmer, A. P.; Fabel, D.; Medialdea, A.; Martin, J.R.V. 2019. Glacial lake evolution and Atlantic-Pacific drainage reversals during deglaciation of the Patagonian Ice Sheet. Quaternary Science Reviews 203: 102-127. doi: https://doi.org/10.1016/j.quascirev.2018.10.036

Turner, K.J.; Fogwill, C.J.; McCulloch, R.D.; Sugden, D.E. 2005. Deglaciation of the eastern flank of the North Patagonian Icefield and associated continental-scale lake diversions. Geografiska Annaler, Series A: Physical Geography 87 (2): 363-374. doi: https://doi.org/10.1111/j.0435-3676.2005.00263.x

Uppala, S.M.; Kållberg, P.W.; Simmons, A.J.; Andrae, U.; Da Costa Bechtold, V.; Fiorino, M.; Gibson, J.K.; Haseler, J.; Hernandez, A.; Kelly, G.A.; Li, X.; Onogi, K.; Saarinen, S.; Sokka, N.; Allan, R.P.; Andersson, E.; Arpe, K.; Balmaseda, M.A.; Beljaars, A.C.M.; Van De Berg, L.; Bidlot, J.; Bormann, N.; Caires, S.; Chevallier, F.; Dethof, A.; Dragosavac, M.; Fisher, M.; Fuentes, M.; Hagemann, S.; Hólm, E.; Hoskins, B.J.; Isaksen, L.; Janssen, P.A.E.M.; Jenne, R.; Mcnally, A.P.; Mahfouf, J.F.; Morcrette, J.J.; Rayner, N.A.; Saunders, R.W.; Simon, P.; Sterl, A.; Trenberth, K.E.; Untch, A.; Vasiljevic, D.; Viterbo, P.; Woollen, J. 2005. The ERA-40 re-analysis. Quarterly Journal of the Royal Meteorological Society 131. doi: https://doi.org/10.1256/qj.04.176

Valet, J.P.; Meynadier, L.; Guyodo, Y. 2005. Geomagnetic dipole strength and reversal rate over the past two million years. Nature 435: 802-805. doi: https://doi.org/10.1038/nature03674

Vásquez, A.; Flores-Aqueveque, V.; Sagredo, E.; Hevia, R.; Villa-Martínez, R.; Moreno, P.I.; Antinao, J.L. 2022. Evolution of Glacial Lake Cochrane During the Last Glacial Termination, Central Chilean Patagonia (47°S). Frontier in Earth Sciences 10. doi: https://doi.org/10.3389/feart.2022.817775.

Manuscript received: February 28, 2022; revised/accepted: June 14, 2022; available online: September 30, 2022.